

# Investigation of the Effective Parameters on the Preparation of Ammonium Perchlorate Particles Using a Cooling Crystallization Process

Seyed Ghorban Hosseini,<sup>\*,[a]</sup> Meysam Nouri,<sup>[a]</sup> Mohammad Mahdi Bahri,<sup>[a]</sup> and Esmail Bazrafshan<sup>[a]</sup>

**Abstract:** Ammonium perchlorate is one of the most important and applicable oxidizers used in solid propellants. Also, the morphology of ammonium perchlorate particles is an effective parameter in the production of propellants. In the current research, the preparation of ammonium perchlorate using the cooling crystallization method was studied. Four parameters including the rate of cooling, mixing patterns, agitator speed, and surfactant were considered in cooling crystallization of ammonium perchlorate. Nine tests were carried out based on the Taguchi experimental design method. The morphology of the obtained crystals was analyzed by optical microscope and MIP 4 student software.

The size distribution of the particles was modeled using the Rosin-Rammler method. Obtained results illustrated that the surfactant had the most effect with the value of 70.7% and the agitator speed, flow pattern, and cooling rate had fewer effects on the morphology with the values of 25.8%, 2.9%, and 0.2%, respectively. The optimal amount of sphericity obtained by the Taguchi method was 0.77 which was verified by the experimental result of 0.76. The roundness and aspect ratio values for the optimal crystal were 0.79 and 1.40 respectively. Applying the Rosin-Rammler model showed that the homogeneity factor of size distribution was 2.22 for the optimal crystals.

**Keywords:** Cooling crystallization · Morphology · Ammonium perchlorate · Rosin-Rammler · Particle size distribution

## 1 Introduction

Rheological and viscoelastic characteristics of a solid propellant are affected by several parameters including particle shape, particle size, binder, and the nature of particles [1,2]. Ammonium perchlorate with a crystallized structure is a strong oxidizer like the other perchlorates [3]. The main part of the propellants (about 90%, volumetric) consists of an oxidizer. Because some of the solid propellants are used for providing flowable slurry and casting into different geometry of grains, the above-mentioned percentage is much less [4]. The performance of the oxidizer used in the formulation may be improved by enhancing the sphericity and smoothness of the particles due to viscosity reduction as the particles slip on each other more easily [5]. Needle-like and plate crystals cause more processing problems. These types of crystals usually show greater filtration resistance and are less flowable compared to the cubic type [6]. The particles with rough and unpredictable shapes are usually broken while slipping [7] and the number of broken particles increases during the slurry process production at a higher rate of mixing which increases the slurry viscosity [8]. Spherical geometry is the best shape to reduce the viscosity while improving a condition that increases the solid content. Other advantages of spherical geometry of particles are the capability of compressing and having higher density [9,10], more fluency, and less breaking contact with each other in an equal volume [11].

Although many researchers studied the crystallization process, less attention has been paid to the crystallization of AP. In the following, some research performed on the crystallization of AP using a different method to obtain modified morphologies is presented. Tai and Cheng [12] produced AP crystals using the anti-solvent method in which the pressure of the system containing AP was increased by introducing CO<sub>2</sub> gas to it and then the crystals were formed by a sudden reduction of pressure. AP crystals produced by this method were polyhedrons, plates, needles, and whiskers with larger sizes concerning the conventional processes of solution crystallization. Li et al. [13] used a ceramic membrane for the solvent and anti-solvent method. Their method was intended to control the morphology and shape of the AP crystals bypassing the saturated solution through a membrane placed in the anti-solvent container. Based on the results, different types of micro-sized AP crystals with different morphologies were obtained including polyhedral-like, quadrate-like to rod-like. They reported that a higher volume ratio of anti-solvent to solvent, higher feeding pressure, and higher temperature caused smaller particle size. Özkar et al. [14] studied the growth of

[a] S. G. Hosseini, M. Nouri, M. M. Bahri, E. Bazrafshan  
Faculty of Chemistry and Chemical Engineering,  
Malek Ashtar University of Technology,  
P. O. Box 16765-3454, Tehran, Iran  
\*e-mail: hoseinitol@yahoo.com

the AP crystals formed through a fluidized bed crystallizer and cooling crystallization method in a pure and sodium chloride solution at different degrees of supersaturation. They concluded that the presence of sodium chloride in the solution reduced the growth and dissolution rates of AP crystals. Based on their results, diffusion and combination of diffusion and integration steps were the controlling mechanisms of the AP crystal growth in pure and sodium chloride solution, respectively. Rogers and Murphy [15] produced AP crystals using the spray-freezing method that involved passing AP solution containing surfactant over a cooling organic liquid to form frozen droplets. The produced AP crystals had mean diameters of less than 1 micron and were especially desirable in the production of solid rocket propellants. Özkar et al. [16] used MSMPR (Mixed-Suspension, Mixed-Product-Removal) crystallizer in the cooling crystallization method to produce AP crystals in presence of NaCl. Their results showed that plate and raked shape crystals were formed in the fluidized bed crystallizer while using NaCl inhibited the formation of raked shape crystals. Tsuzuki et al. [17] investigated the effect of ethylene glycol on the AP crystals growth. They added a saturated aqueous solution of AP to an organic solvent at 333 K and then cooled to 273–275 K which led to AP crystallization with modified geometry. According to the results, thermal decomposition and ignition behavior of modified AP were superior to those of standard AP. The burning rate of the propellant containing modified AP was higher than propellant with standard AP. Lakshmi et al. [18] studied the effect of different parameters on AP crystals. The results showed that increasing the agitator speed will enhance the sphericity. Also, re-crystallization occurred by the low rate of cooling as was observed that the crystals formed at 600 rpm and low cooling rate were more smooth and spherical.

As mentioned previously, controlling the crystal growth especially in solvent and anti-solvent method is difficult; therefore, in the current study, to better control crystal growth, the cooling crystallization method was chosen for producing the AP crystals. Also, different cooling procedures, surfactants, and unknown conditions affecting crystallization have motivated much research in this field. In the present study, effect of four parameters including cooling rate, mixing pattern, surfactant, and agitator speed on the AP crystallization was investigated.

## 2 Materials and Methods

Taguchi method was used for experimental design by using the Qualitek 4 software. The cooling rate was set in three different linear rates including quick, slow, and moderate. Using two draft tube models, three different patterns of mixing were considered and the agitator speed was determined experimentally. The effect of surfactant was investigated in three states of surfactant-free and two different percentage contents of solution.

Approximately 1.3 L of the saturated solution was prepared by mixing 1.0 L of distilled water with 493 g of AP at 60 °C. The obtained solution was maintained in a 4.0 L volume steel container which was kept at a temperature 5 °C higher than the solution temperature. The temperature of the container was controlled by water circulating in a coil passing through the bath. The distance of the impeller from the bottom of the container was fixed in all the tests. Sampling was performed after cooling the solution to 30 °C and then the samples were dried in an oven at 80 °C. A schematic of the crystallization process is depicted in Figure 1.

Cooling rates were set to three values of 0.500 °C/min, 0.250 °C/min (Figure 2) and 0.125 °C/min. The agitator speeds were set to 600, 500, and 400 rpm. Sodium dodecyl sulfate (SDS,  $\text{NaC}_{12}\text{H}_{25}\text{SO}_4$ ) was used as a surfactant at three different concentrations of 0.0, 0.1, and 0.2 weight percentage.

To induce a different pattern of fluid mixing, three different procedures including mixing with impeller (fluid pattern A), draft tube (fluid pattern B), and a modified draft tube (fluid pattern C) were used. Mixing the components by the impeller leads to a condition in which the crystal particles move with the impeller speed. In this condition, the mixing efficiency will reduce. Using a draft tube eliminates the mentioned problem of the impeller and forces the fluid to be mixed vertically and laterally due to the induced suction of impellers and baffles, respectively. Particle size growth makes itself heavier, hence, the particle precipitates and cannot remain floated in the mixture. To omit this problem, a pressure difference was induced by reducing the cross-section area of the cylinder. The temperature of the heating bath was kept about 5 °C higher than the solution in the container to prevent the nucleation of the AP. The container was fully insulated to achieve a minimum heat loss.

The data presented in Table 1 and 2 show the factors and levels of the experimental design. In this study, AP crystals were observed by an optical microscope (UNICO, model: G380) and then the obtained data were analyzed by MIP 4 student software to determine the sphericity and aspect ratio of the crystals. The size distribution of the crystals was determined using Laser Micron Sizer (model: LMS-30) instrument.

The sphericity lies between 0.00 and 1.00 while the amount closer to 1.00 is more favorable. The aspect ratio may help to determine the sphericity more accurately. A closer amount of aspect ratio to 1.00 shows the uniform multidimensional growth of the crystals. Therefore, considering these parameters and their related amount determine which particle has uniform spherical shape. The optimum shape of the crystals is spherically shaped and has sphericity between 0.70 and 1.00 [19].

MIP 4 student is professional software for image analysis. This software output data is presented in html format. The obtained images of the prepared samples are pre-

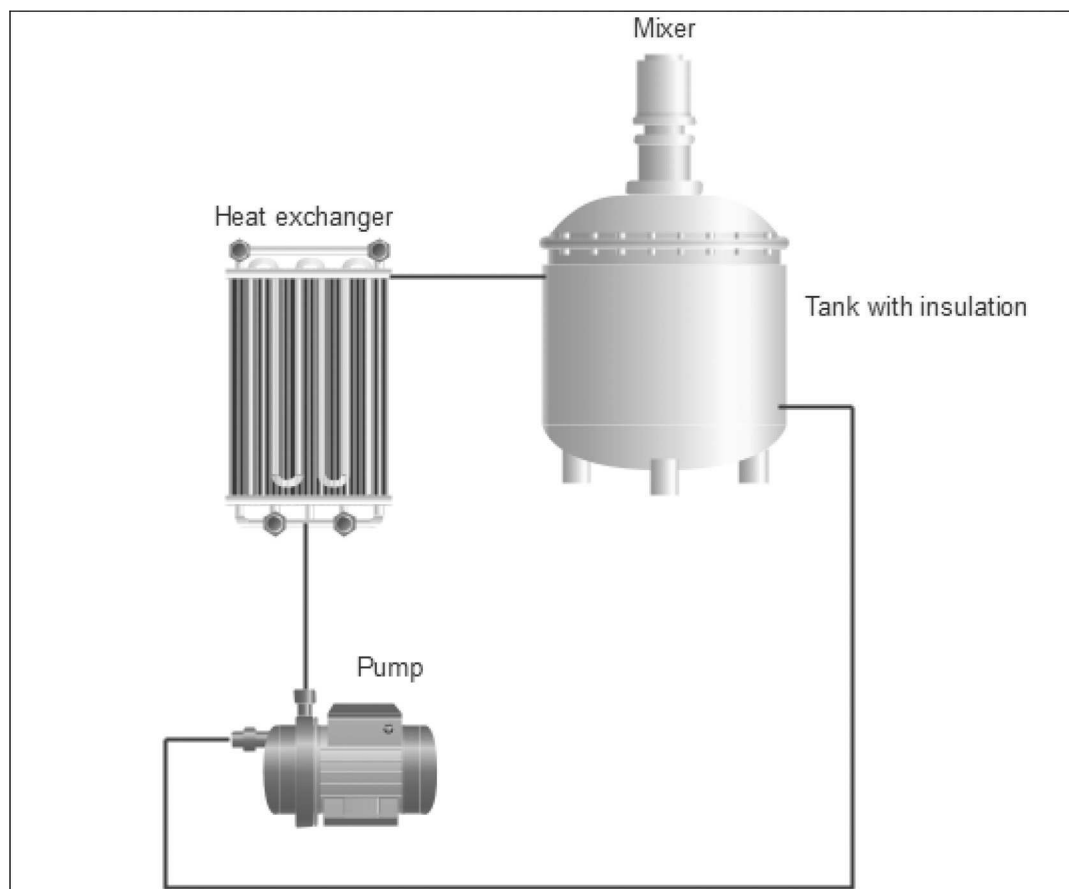


**Figure 1.** Schematic diagram of the crystallization process and the equipment used for the process.

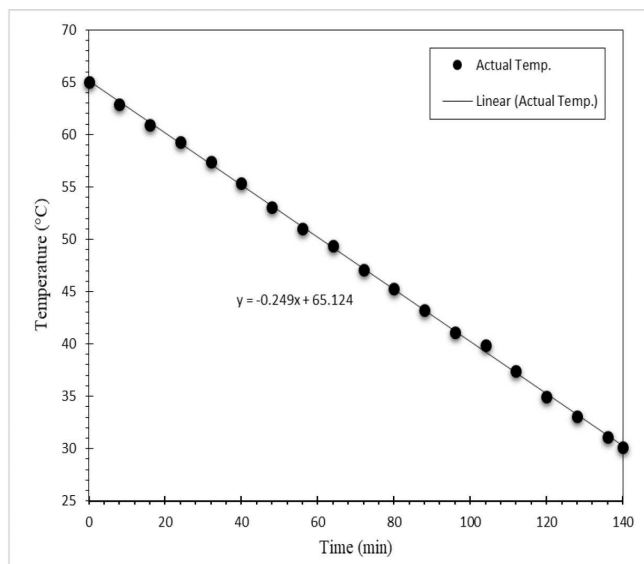


**Figure 2.** Cooling rate for the performed experiment and their comparison with the optimal cooling rate of  $0.250^{\circ}\text{C}/\text{min}$ .

sented in the results and discussion section (<http://metsofts.ir/download-mipstudent/>).

The composition and structure of commercial (MS) and produced AP particles at optimum condition (MB) were determined by the X-ray diffraction (XRD) analysis method. XRD analyses of the sample were carried out using a Philips diffractometer (Model TM-1800). Nickel filtered  $\text{Cu-K}\alpha$  radiation source was used to produce X-ray ( $\lambda = 1.542 \text{ \AA}$ ), and scattered radiation was measured with a proportional counter detector at a scan rate of  $4^{\circ}\text{min}^{-1}$ . The scanning angle was from  $10^{\circ}$  to  $90^{\circ}$ , operating at a voltage of 40 kV applying a potential current of 30 mA.

## 3 Results and Discussion

### 3.1 Influence of Crystallization Parameters on Crystal Formation

In this work, the effect of agitator speed and surfactant was the same as the results obtained by Lakshmi et al. [18]. By increasing the agitator speed, the shape of the crystals was modified, and adding the surfactant to the initial solution enhanced the sphericity. In comparison with the results ob-

**Table 1.** Taguchi L-9 orthogonal array design and specification of the prepared ammonium perchlorate particles.

| Experiment | Cooling rate (°Cmin <sup>-1</sup> ) | Agitator rpm | SDS (%) | Fluid pattern | Sphericity | Aspect ratio | Roundness | Average Size (μm) |
|------------|-------------------------------------|--------------|---------|---------------|------------|--------------|-----------|-------------------|
| 1          | 0.125                               | 400          | 0.0     | A             | 0.61       | 1.29         | 0.77      | 306.4             |
| 2          | 0.125                               | 500          | 0.1     | B             | 0.70       | 1.29         | 0.81      | 48.4              |
| 3          | 0.125                               | 600          | 0.2     | C             | 0.75       | 1.40         | 0.81      | 49.0              |
| 4          | 0.250                               | 400          | 0.1     | C             | 0.72       | 1.44         | 0.72      | 51.5              |
| 5          | 0.250                               | 500          | 0.2     | A             | 0.69       | 1.52         | 0.70      | 50.8              |
| 6          | 0.250                               | 600          | 0.0     | B             | 0.66       | 1.10         | 0.88      | 247.4             |
| 7          | 0.500                               | 400          | 0.2     | B             | 0.69       | 1.44         | 0.74      | 65.6              |
| 8          | 0.500                               | 500          | 0.0     | C             | 0.63       | 1.18         | 0.83      | 223.1             |
| 9          | 0.500                               | 600          | 0.1     | A             | 0.75       | 1.45         | 0.74      | 85.9              |

**Table 2.** The various parameters selected and their respective levels in the present experimental design.

| Process parameter                 | Symbol | Level 1 | Level 2 | Level 3 |
|-----------------------------------|--------|---------|---------|---------|
| Cooling rate/°Cmin <sup>-1</sup>  | C      | 0.125   | 0.250   | 0.500   |
| Stirring speed of the mixture/rpm | R      | 400     | 500     | 600     |
| SDS/wt. %                         | S      | 0.0     | 0.1     | 0.2     |
| Fluid pattern                     | F      | A       | B       | C       |

tained from solvent and anti-solvent methods, the shape of the crystals was more favorable and spherical.

Some images of the AP crystals have been shown in Figure 3. Adding the surfactant to the solution led to form smaller particles with a smoother surface (Figure 3c). In the cases where the cooling rate was low and no surfactant was used, the particles were bigger (Figure 3a). The shapes of the crystals were analyzed by the images and MIP 4 student software. The results of the analysis have been presented in Table 1.

The results were analyzed in detail using Taguchi method and presented in Figure 4. As can be seen, the surfactant is the most effective parameter with an effectiveness of 70.7%. After that, agitator speed, fluid pattern, and cooling rate with the effectiveness of 25.7%, 2.9%, and 0.2% were in the next levels, respectively. Because of the low effectiveness of the cooling rate, it can be neglected. Therefore, at equal conditions, performing the experiments at any cooling rate results in similar sphericities.

The main influence of each parameter has been presented in Table 3. Analyzing the data by Taguchi method

**Table 3.** Optimal amount of each parameter and their related predicted value.

| Parameter     | 1     | Level 2 | 3     | L <sub>2</sub> -L <sub>1</sub> |
|---------------|-------|---------|-------|--------------------------------|
| Cooling rate  | 0.690 | 0.690   | 0.694 | 0.000                          |
| Agitator rpm  | 0.673 | 0.675   | 0.724 | 0.002                          |
| SDS           | 0.636 | 0.725   | 0.711 | 0.088                          |
| Fluid pattern | 0.685 | 0.685   | 0.702 | 0.000                          |

showed that the cooling rate parameter had less effectiveness value, so it was omitted. Then according to Fischer test, the amounts of F for surfactant, agitator speed, and fluid pattern were 421.8, 153.7, and 17.8 respectively.

Referring to the data reported by Roy [20], the values of F were determined for different amounts of certainties. If the presented data by the software is more than the corresponding data in references, then the obtained result will be reliable for each F value. The calculation is started by the highest value of confidence. The F<sub>99%</sub>, F<sub>95%</sub>, and F<sub>90%</sub> values are 99, 19, and 9 respectively. As can be seen, only at an F value of 90%, all of the three parameters are reliable.

The optimal conditions for experimenting were determined by the Taguchi method. The reported data revealed that the optimal condition occurred at an agitator speed of 600 rpm, 0.1 wt. % of surfactant, and using the draft tube for better mixing and fluid pattern. The parameter of the cooling rate due to its neutrality toward the results was omitted.

The predicted values of sphericity, roundness, aspect ratio, and average particle size at the proposed optimal experiment condition, were 0.77, 0.79, 1.41, and 42.1 respectively. To evaluate the suggested results from software analysis, experiments were carried out at optimum conditions (mixing speed of 600 rpm, 0.1 wt. % of surfactant, the cooling rate of 0.500 °C/min, and using draft tube). Based on the obtained results from the experimental analysis at the optimal experiment condition, the values of sphericity, roundness, aspect ratio, and average particle size were 0.76, 0.81, 1.38, and 43.7 respectively. The difference of the experimental value of sphericity with the predicted value obtained by Taguchi method was about 0.01.

The confidence interval determines whether the obtained answer is reliable or not. Confidence interval is determined by equation (1) as follows:

$$C.I. = \pm \sqrt{(F(1, n) \times \frac{V_e}{N_e})} \quad (1)$$

Where the V<sub>e</sub> is the variance of error, N<sub>e</sub> is obtained by dividing number of experiments to the sum of the average degree of freedom and degree of freedom of residuals, and

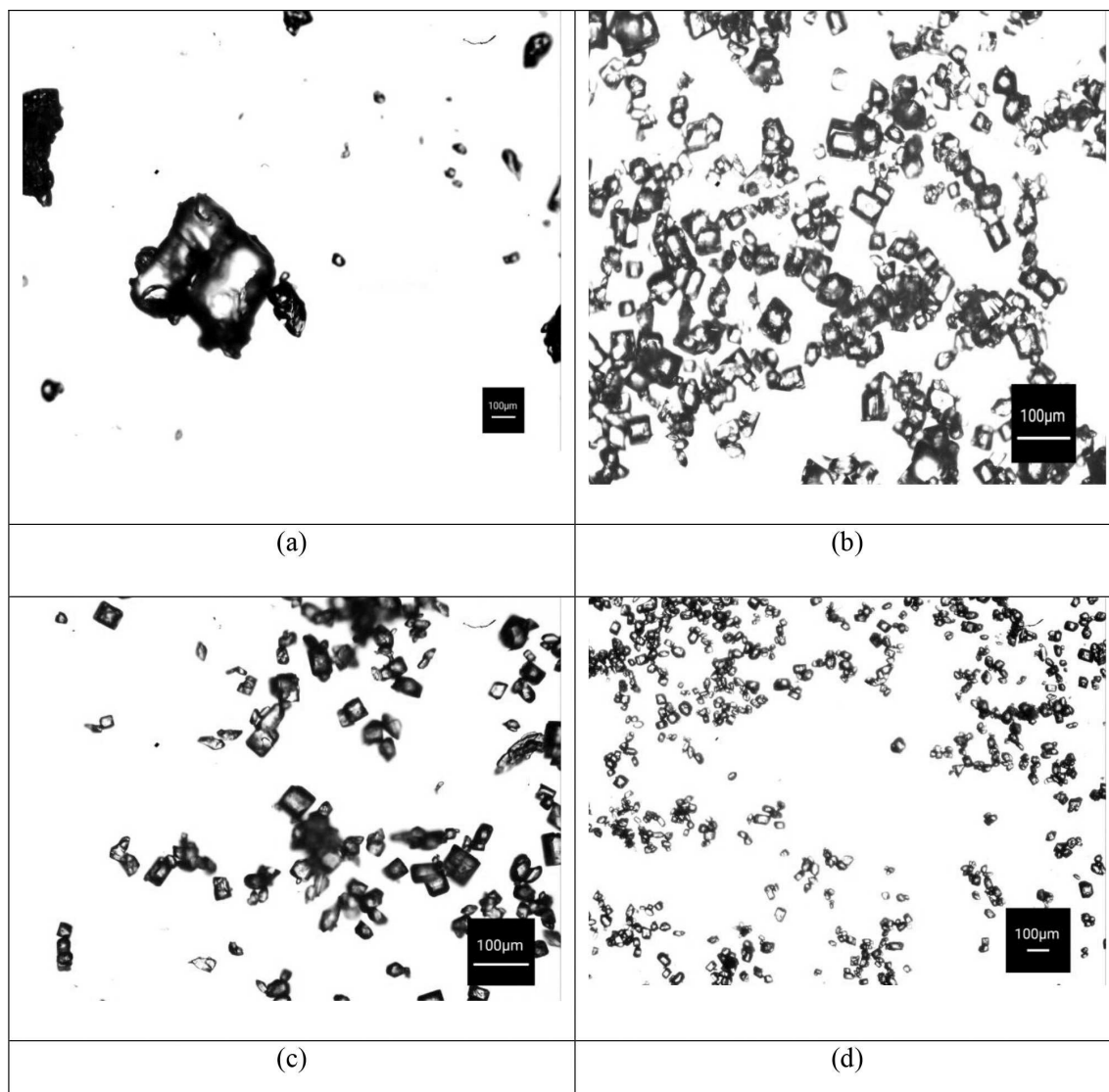


**Figure 3.** The image of crystals obtained from different runs of AP crystallization process, (a) experiment 1, (b) experiment 2, (c) experiment 3 and (d) experiment 4. (test conditions).

$F(1,n)$  is obtained from the F tables in which  $n$  is the residuals degree of freedom [20].

The confidence interval for the optimal response was calculated by equation 1. The error variance was calculated 0.001 after omitting the cooling rate and the  $N_e$  value became 1.29. The value of  $F(1, n)$  at  $n$  times more than 2 equals 8.5, hence, by use of equation (1) the confidence interval for the optimal value predicted by the Taguchi method is 0.08. Accordingly, the optimal value should lie between 0.69 and 0.85 which verifies the confidence of obtained experimental results.

Rosin and Rammler presented a relation to determine the size distribution of particles with the suitable response and negligible error [21–23]. Rosin Rammler equation is as follows:

$$Y = 1 - \exp\left(-\left(\frac{x}{x_0}\right)^n\right) \quad (2)$$

Where  $Y$  is the mass fraction smaller than a given diameter  $x$ ,  $x_0$  is the characteristic size of the particles ( $1-1/e = 0.632$ ) defined as the size of the smaller particles and  $n$  is the Rosin-Rammler exponent (uniformity coefficient) illustrating the slope of the linearized form of equation (2) as presented by equation (3):

$$\log\left[\ln\left(\frac{1}{1-Y}\right)\right] = n \log(x) + c \quad (3)$$

The  $n$  and  $x_0$  known as the Rosin-Rammler coefficient are easily obtained by linear regression. The higher value of

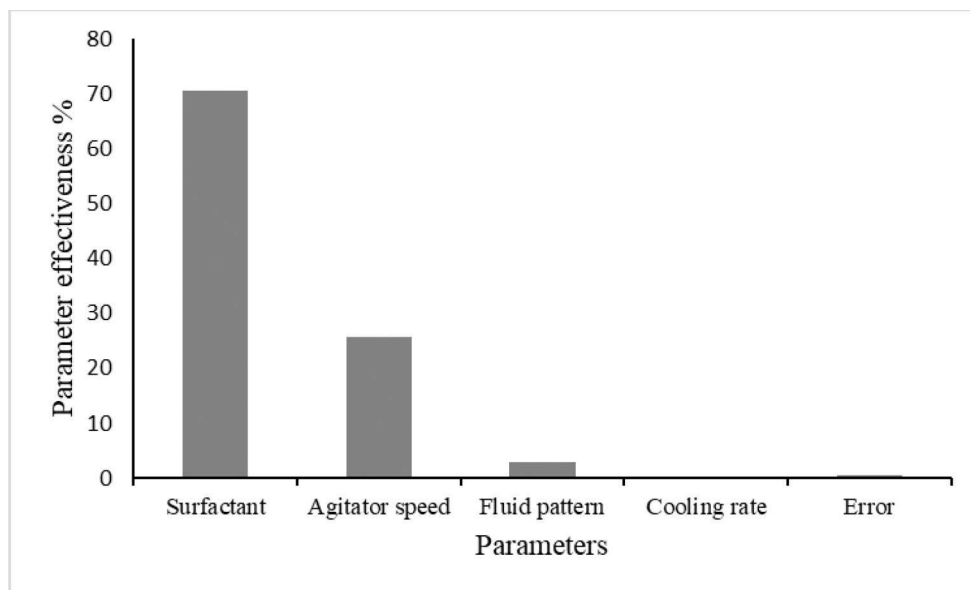


**Figure 4.** Effectiveness of different parameters on the crystals sphericity.

**Table 4.** Uniformity coefficient and error values determined by regression of Rosin-Rammler model.

| Experiment | Uniformity coefficient ( $n$ ) | Determination coefficient ( $R^2$ ) |
|------------|--------------------------------|-------------------------------------|
| 1          | 0.63                           | 0.74                                |
| 2          | 1.79                           | 0.82                                |
| 3          | 2.42                           | 0.91                                |
| 4          | 2.25                           | 0.97                                |
| 5          | 2.16                           | 0.95                                |
| 6          | 0.81                           | 0.89                                |
| 7          | 2.24                           | 0.99                                |
| 8          | 0.74                           | 0.77                                |
| 9          | 3.11                           | 0.94                                |

$n$  is favorable as it reveals the closer spread of particle size [24, 25].

According to the Rosin-Rammler equation and the data obtained from the particle size distribution instrument, a fixed exponent ( $n$ ) can be calculated. Different values of calculated exponent have been presented in Table 4. The higher values of exponent  $n$  show the more favorable size distribution of the particles. As the reported data in Table 4 reveal, in the cases where the surfactant was used, higher values of  $n$  were obtained compared to experiments 1, 6, and 8 without surfactant.

The size distribution of the particles formed under the optimal condition has been shown in Figure 5. The result in Figure 5 shown, the exponent  $n$  is equal to 2.22 for optimal

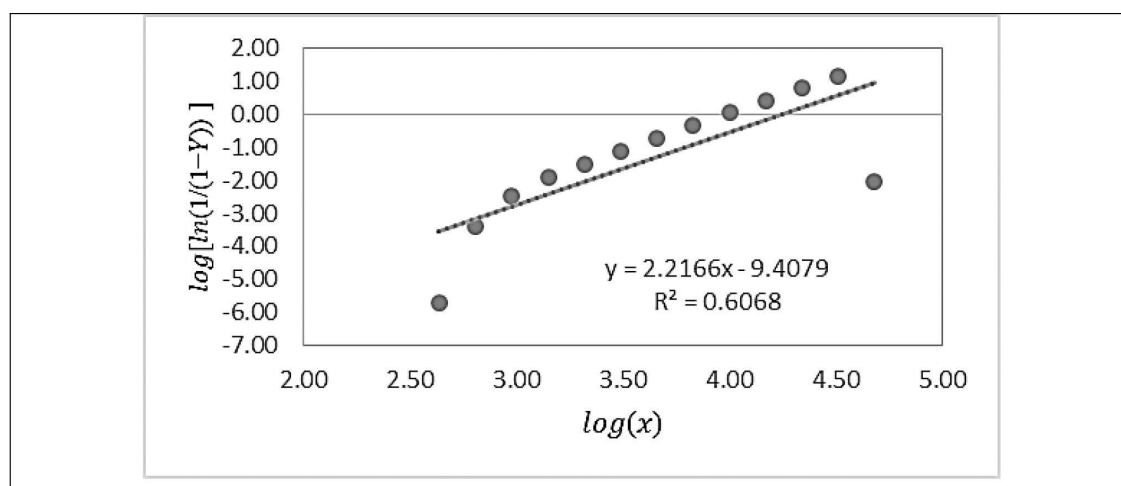


**Figure 5.** Plot of the size distribution of the optimal particles determined from Rosin-Rammler model.



condition sample and shows a more appropriate size distribution compared to other samples. Although, based on summarized results in Table 4, the value of  $n$  for experiment sample 9 is equal to 3.11 and indicates a more favorable size distribution optimization in the current study were done respect to the sphericity of obtained particles and values of sphericity for the experiment sample 9 is 0.75 which is lower than that the value of optimal experiment sample (0.76).

As the experimental results show (experiments 3, 5, and 7), by increasing the surfactant amount in the solution, the aspect ratio has been increased. The surfactant presence induces the crystal elongation rather than widening the particles and may affect each particle differently. Also, SDS improved the sphericity considerably compared to the states without the SDS (experiments 1, 6, and 8).

The agitator speed has a great effect on the sphericity of the particles so that by increasing the agitator speed (experiments 3, 6, and 9), the sphericity increases. This event is due to the better mixing at high speeds and mechanical erosion of the particles due to the more sudden contacts between them. The aspect ratio of the particles decreases by increasing the agitator speed. According to the results, the mixing pattern and cooling rate have a negligible effect on the crystal in comparison with the surfactant effect. The mixing pattern is the next factor that is being analyzed. The effect of this factor and the rate of cooling are very poor. This is due to the effect of surfactant that reduces their effectiveness.

Based on the results, the sphericity of all samples was favorable. The mixing pattern and presence of the surfactant in the solution had a considerable effect on the final results. The sphericity was directly increased by improving the mixing pattern and increasing the agitator speed. Adding the surfactant to the crystallization environment helped to control the crystal's growth and improved the sphericity. The lower cooling rate provided enough time for the formation of crystals and therefore improved the shape of crystals.

The presence of the surfactant reduces the surface tension which leads to a reduction in free energy. Therefore, the solution quickly reaches the supersaturation state and the crystals appear in the solution which enhances the nucleation and decreases the size of the nucleons. The mentioned point is verified by the image of crystals. Accordingly, in the case of using surfactant due to the reduction in

surface tension, the rate of the nucleation was increased and smaller crystals were formed by increasing the surfactant content of the solution. Also, surfactant led to the formation of a smoother crystal surface.

The rate of cooling affected the size of the particles so that by reducing the cooling rate, bigger particles were formed. This happened as enough time was provided for the smaller particle to sediment on the bigger ones at the supersaturation state while it limited the formation of new crystals. The draft tube improved the mixing through helping the particles to move with different speed compared to the impeller.

The agitator speed and appropriate mixing have positively affected the size distribution. This may be explained by the decrease of nucleation and growth of the existing crystals where the mixing is favorable. Also, very high agitator speed adversely affects the size distribution as the impeller may break the big size crystals. The cooling rate affects both the size and size distribution of the crystals. Because of the surfactant presence in the crystallization environment, the effect of other parameters is negligible.

### 3.2 DSC-TG and XRD Analysis

The "MS" represents the primary and commercial samples and the "MB" represents the optimized produced sample. The amount of energy released ( $\Delta H$ ), starting, peak, and final decomposition temperatures ( $T_o$ ,  $T_p$ , and  $T_e$ ) have been listed in Table 5. A peak also is seen in the 240 °C to 250 °C temperature range in the DSC diagram that is related to AP restructuring from orthorhombic to cubic due to the rotation of perchlorate ions and required heat from 85 J/g to 88 J/g (Figure 6).

The data presented in Table 5 show that the significant changes in the amounts of absorbed and total released energy are not observed in the two samples. Reported temperatures have increased.

The composition and structure of commercial (MS) and produced AP particles at optimum condition (MB) were determined by the X-ray diffraction (XRD) analyses method and results were illustrated in Figure 7. The XRD patterns of MS and MB samples were broadly similar to that of the standard AP (ASTM pattern reference code: 00-008-0451) pattern [18]. According to the above record in the ICDD database, nine main peaks appear for AP particles at 15.3°,

**Table 5.** Characterization DSC-TG test for optimized and commercial samples.

| Sample No. | Decomposition phenomenon      | $T_o$ /°C | $T_p$ /°C | $T_e$ /°C | $\Delta H$ /Jg <sup>-1</sup> |
|------------|-------------------------------|-----------|-----------|-----------|------------------------------|
| MB         | 1 <sup>st</sup> decomposition | 312.5     | 325.0     | 337.7     | 368.3                        |
|            | 2 <sup>nd</sup> decomposition | 410.9     | 437.2     | 446.1     | 497.8                        |
| MS         | 1 <sup>st</sup> decomposition | 271.6     | 287.8     | 301.9     | 313.5                        |
|            | 2 <sup>nd</sup> decomposition | 402.3     | 437.8     | 445.1     | 577.1                        |

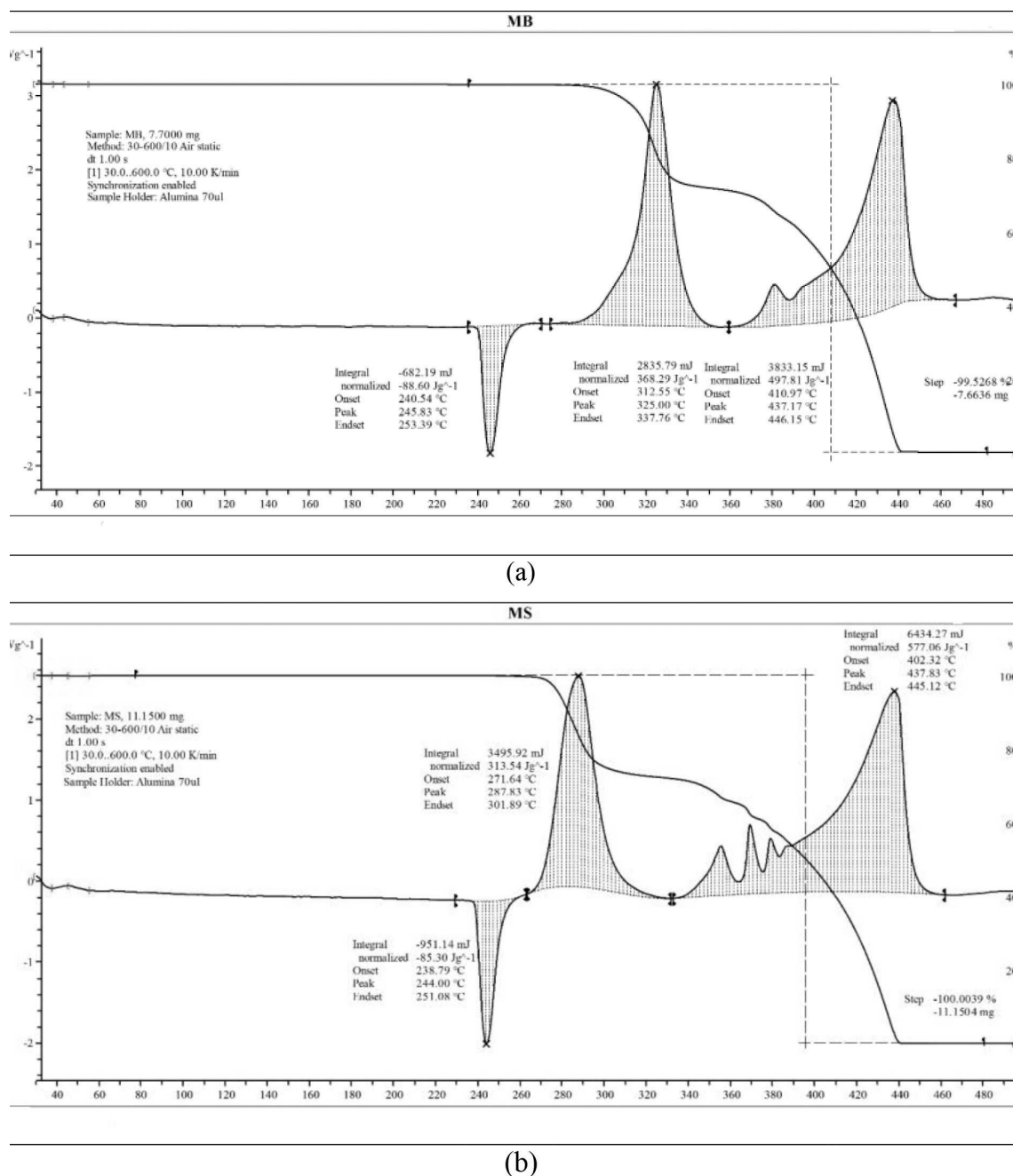


**Figure 6.** DSC-TG analysis performed for (a) optimized sample and (b) commercial sample.

19.4°, 22.7°, 23.9°, 24.6°, 27.4°, 30.1°, 30.8° and 34.6° of  $2\theta$ . The sharp diffraction peaks were observed at  $2\theta$  angles of 19.4°, 22.7°, 23.9°, 24.6°, 27.4°, and 34.6° respectively corresponded to (001), (201), (002), (210), (211), and (212) crystal plane of both AP particles. However the summarized result in Figure 7.b was proven that in MB sample, 011 crystalline planes have strongly degraded and growth has decreased in this plane. Also in 002, 211 crystalline planes growth has increased concerning the MS ones without using any surface-active agent (Figure 7.a). The obtained crystallinity re-

sult confirmed that the surface-active agent could change the growth of different planes and produced a crystalline sphere with a combination of other affecting factors.

## 4 Conclusion

Analysis of the experimental results by the Taguchi method showed that the surfactant with 70.7% of effectiveness is the most vital parameter and may affect the multidimen-



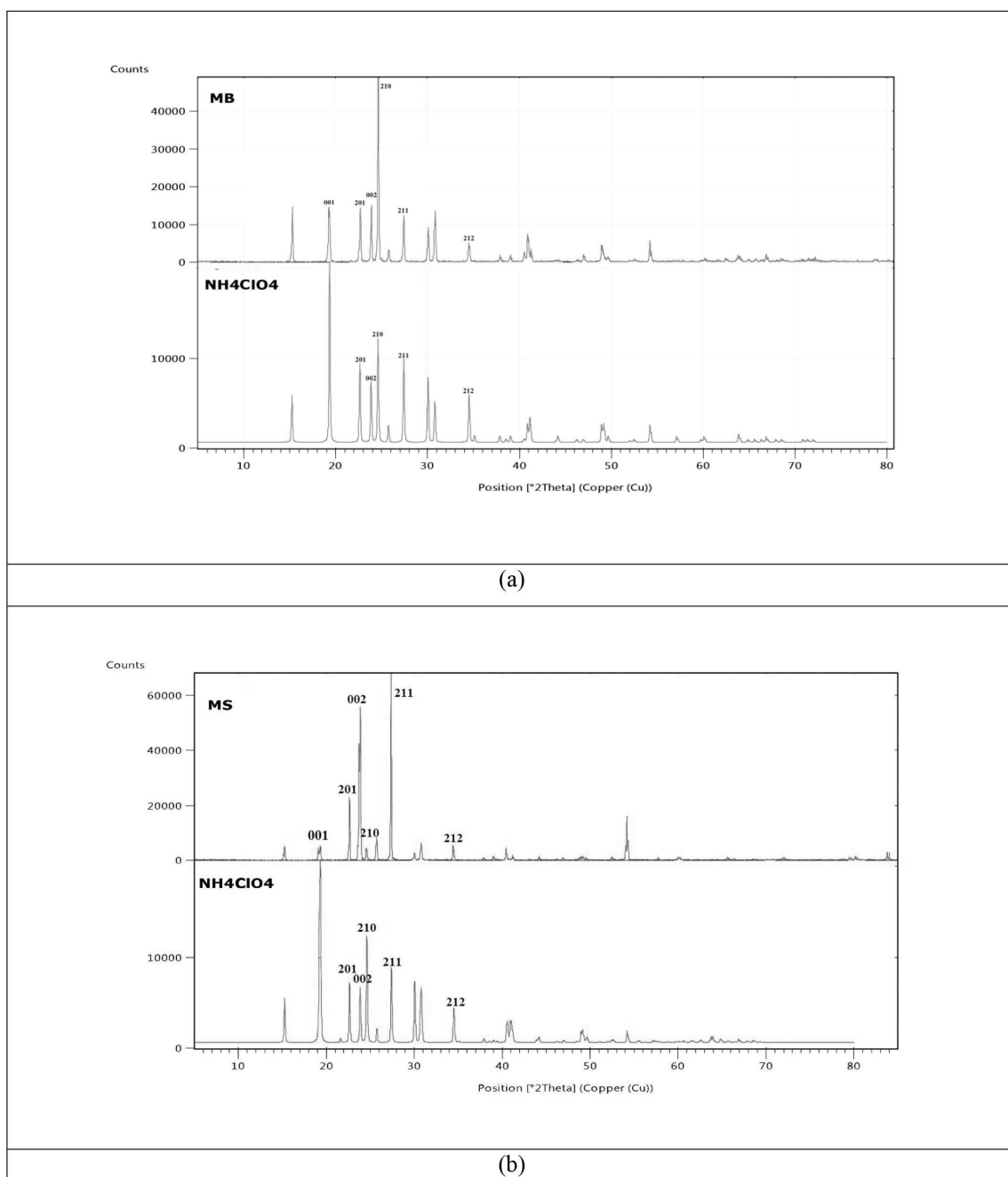


**Figure 7.** The XRD analysis performed for (a) commercial and (b) optimized samples.

sional growth of the crystal. The agitator speed positively affected the crystal's sphericity up to 25.7%. The sphericity of the crystals was also improved by approximately 2.9% by more favorable mixing. Better mixing leads to the growth of the crystals floating in the solution. Oppositely, unfavorable mixing may lead to precipitation of crystals and the formation of new nucleons that decrease the quality of size distribution and asymmetric growth of the precipitated crystals. The effect of cooling rate was neglected as it approximately showed no effect on particles shape and size.

The analysis of the size distribution results revealed that the surfactant present in the solution improves the size distribution while in the case where no surfactant was used the uniformity coefficient ( $n$ ) was determined 0.63, 0.81, and 0.74 for the experiment number of 1, 6 and 8, respectively.

## Data Availability Statement

The authors confirm that the data supporting the findings of this study are available within the article.

## References

- [1] R. Muthiah, V. Krishnamurthy, B. Gupta, Rheology of HTPB propellant. I. Effect of solid loading, oxidizer particle size, and aluminum content, *J. Appl. Polym. Sci.* **1992**, *44*, 2043.
- [2] C. Boyars, K. Klager, *Propellants manufacture, hazards, and testing*, ACS Publications, **1969**.
- [3] A. Davenas, *Solid rocket propulsion technology*, Newnes, **2012**.
- [4] G. A. Fluke, *Composite solid propellant processing techniques*, ACS Publications, **1969**.
- [5] M. J. Rhodes, *Introduction to particle technology*, John Wiley & Sons, **2008**.
- [6] H.-H. Tung, E. L. Paul, M. Midler, J. A. McCauley, *Crystallization of organic compounds: an industrial perspective*, John Wiley & Sons, **2009**.
- [7] J. F. Gregory, R. P. Levey, Method for preparation of spherical UO, US3037840 A, **1962**.
- [8] S. Amini, M. Keshavarz, F. M. Ghorbani, A. Mousaviazar, M. Aghayari, Effect of Double Sizes (Coarse/Fine) Ammonium Perchlorate on the Viscosity of Composite Solid Propellant, *J. Energ. Mater.* **2014**, *9*, 61.
- [9] N. Saito, M. Yokota, T. Fujiwara, N. Kubota, Liquid inclusions in crystals produced in suspension crystallization, *Chem. Eng. J.* **2000**, *79*, 53.
- [10] A. S. Myerson, R. Ginde, in *Handbook of industrial crystallization*, Elsevier, **2002**, pp. 33.
- [11] R. D. Nelson, *Dispersing powders in liquids*, Elsevier, **2012**.
- [12] C. Y. Tai, C.-S. Cheng, Supersaturation and crystal growth in gas anti-solvent crystallization, *J. Cryst. Growth* **1998**, *183*, 622.
- [13] Z. Ma, C. Li, R. Wu, R. Chen, Z. Gu, Preparation and characterization of superfine ammonium perchlorate (AP) crystals through ceramic membrane anti-solvent crystallization, *J. Cryst. Growth* **2009**, *311*, 4575.
- [14] S. Tanrikulu, I. Eroğlu, A. Bulutcu, S. Özkar, The growth and dissolution of ammonium perchlorate crystals in a fluidized bed crystallizer, *J. Cryst. Growth* **1998**, *194*, 220.
- [15] R. Rogers, J. Murphy, Method of making ultra-fine ammonium perchlorate particles, US3819336 A, **1974**, 6.
- [16] S. Ü. Tanrikulu, I. Eroğlu, A. Bulutcu, S. Özkar, Crystallization kinetics of ammonium perchlorate in MSMPR crystallizer, *J. Cryst. Growth* **2000**, *208*, 533.
- [17] M. Kohga, H. Tsuzuki, Burning-rate characteristics of composite propellant using ammonium perchlorate modified by ethylene glycol, *J. Propul. Power* **2011**, *27*, 668.
- [18] V. Lakshmi, S. Chakravarthy, A. Rajendran, C. Thomas, Effect of crystallization parameters and presence of surfactant on ammonium perchlorate crystal characteristics, *Part. Sci. Technol.* **2016**, *34*, 308.
- [19] J. Rodriguez, T. Edeskär, S. Knutsson, Particle shape quantities and measurement techniques: a review, *The Electronic journal of geotechnical engineering* **2013**, *18*, 169.
- [20] R. K. Roy, *Design of experiments using the Taguchi approach: 16 steps to product and process improvement*, John Wiley & Sons, **2001**.
- [21] P. Rosin, Laws governing the fineness of powdered coal, *Journal of Institute of Fuel* **1933**, *7*, 29.
- [22] G. Savage, J. Tuck, P. Gandy, G. Trezek, *Significance of Size Reduction in Solid Waste Management*, U. S. Environmental Protection Agency Report, EPA Number: EPA/600/2-83/006, **1983**.
- [23] T. Allen, *Powder sampling and particle size measurement*, Vol. 1, Chapman and Hall, **1997**.
- [24] P. A. Vesilind, The Rosin-Rammler particle size distribution, *Resour. Recovery Conserv.* **1980**, *5*, 275.
- [25] I. Brezani, F. Zelenak, Improving the effectivity of work with Rosin-Rammler diagram by using MATLAB (R) GUI tool, *Acta Montanistica Slovaca* **2010**, *15*, 152.

Manuscript received: November 25, 2020

Revised manuscript received: April 3, 2021

Version of record online: April 23, 2021